Heliyon 9 (2023) e13104

Contents lists available at ScienceDirect

Heliyon

journal homepage: www.cell.com/heliyon

Research article

Cellulose nanocrystals from Siam weed: Synthesis and physicochemical characterization

Joseph K. Ogunjobi [a,*], Adetola I. Adewale [a], Samson A. Adeyemi [b]

[a] Department of Chemistry, Federal University of Technology, PMB 704, Akure, Nigeria
[b] Wits Advanced Drug Delivery Platform Research Unit, Department of Pharmacy and Pharmacology, School of Therapeutic Science, University of the Witwatersrand, Johannesburg, 7 York Road, Parktown, 2193, South Africa

ARTICLE INFO

Keywords:
Biomass
Green solvent
Adsorption
Crystallinity
Waste valorisation
Nanocellulose
Chromolaena odorata
Sustainability
Green extraction

ABSTRACT

The use of biomass for the development of environmentally friendly and industrially useful materials is still attracting global interest. Herein, cellulose nanocrystals were prepared from Siam weed. The production steps involved dewaxing the biomass sample, bleaching treatment, alkali treatment and acid hydrolysis. The resulting cellulose nanocrystals were characterized using Fourier transformed infrared (FTIR) spectroscopy, X-ray diffraction (XRD) spectroscopy, thermogravimetric analysis (TGA), scanning electron microscopy (SEM), transmission electron microscopy (TEM) and dynamic light scattering (DLS) technique. Chemical composition results showed that Siam weed contained 39.6% cellulose, 27.5% hemicellulose, 28.7% lignin and 4.2% extractive. FTIR spectrum confirmed the presence of cellulose and absence of lignin and hemicellulose while XRD analysis revealed that the cellulose nanocrystals have crystallinity index of 66.2% and particle size of 2.2 nm. TGA revealed that thermal stability of raw Siam weed is lower than that of its cellulose nanocrystals due to the presence of the non-cellulosic component with lower temperature of degradation. SEM revealed that degradation of cellulosic chain had occurred. TEM confirmed that the crystal size is in the nanoscale with an average size <100 nm. DLS data revealed a nanocellulose with an average hydrodynamic size of 213 nm and a zeta potential at −9.57 mV.

1. Introduction

Biomass from plant agricultural wastes contains cellulose which is a major constituent chemical found in the cell wall of trees and green plants. Cellulosic agricultural waste is very economical, readily available, non-toxic, renewable, easily processable and biodegradable [1–3]. Cellulose and some of its derivatives are approved by the European Food Safety Authority, Food Standard Agency and the US Food and Drug Administration (FDA) for use as additives in food product [4]. The ability of cellulose to be prepared in nano-metric dimensions has made it attract significant attention in the field of nanotechnology. Nanomaterials have been reported to exhibit remarkable properties due to their possession of high tensile strength, high thermal properties, transparency and flexibility [5]. These properties in turn decides the end-application of nanocellulose in the industry. For instance, nanocellulose is employed as fillers in textile and polymer industry owing to its large surface area [6]. Several nanocellulose materials having increased tensile strength, modulus and rigidity with potential applications in electronic devices, have been prepared from plant materials [7].

* Corresponding author.
E-mail address: jkogunjobi@futa.edu.ng (J.K. Ogunjobi).

https://doi.org/10.1016/j.heliyon.2023.e13104
Received 25 January 2022; Received in revised form 13 January 2023; Accepted 16 January 2023
Available online 20 January 2023

Cellulose nanocrystals (CNCs) are a type of nanocellulose and are mostly prepared by acid hydrolysis [8]. This method helps in hydrolysing the amorphous part of the cellulose while the crystalline part is retained leading to a highly ordered material. CNCs have promising properties, which include high aspect ratio, high tensile strength, high surface area, high crystallinity, supramolecular structure and excellent stiffness. These properties give them the special advantage of application in diverse fields of chemical and engineering science. CNC's properties are source dependent, therefore appropriate cellulosic raw material and suitable extraction procedure must be established based on the needed final CNC properties and applications [9]. CNCs have been effective in several applications, including water and wastewater treatment [10], biomedical engineering [11], energy production [12], drug delivery [13], polymer nanocomposite [14,15], electronics [16,17], among many others. CNC from softwood pulp has demonstrated a striking behaviour that predicted its potential use as carriers in specific drug delivery applications [18]. Hairy CNC from wood pulp had been prepared and used for dye removal due to its excellent bio-adsorptive property [19].

Following the versatility of applications of CNC, there is a growing demand for cellulosic-based chemicals, hence the need to source for more routes to generate cellulose. Recent efforts geared towards obtaining cellulose focus on abundant agricultural wastes in the environment. Isolation of cellulose and CNC from the following agricultural wastes has been reported: rice straw [20], coconut shell [16], ground nut shell [21], walnut shell [22], jackfruit peel [23], corn straw [24], aerial yam [25], bamboo [26] and sisal [27].

Siam weed (SW), also known as *Chromolaena odorata,* is a perennial shrub that originally grows rapidly in South America and Central America but was introduced into the tropical region of Africa, the Pacific and Asia where it has become ubiquitous [28]. It is a common environmental weed occurring mostly in places with high humidity and altitudes less than 2000 m. Presently, SW is undesirable in any area and causes poisoning in livestock if consumed. This weed, as a biomass, has an advantage of being far more abundant in the environment and its availability does not depend on any deliberate cultivation when compared with other agricultural wastes from which cellulose has been previously isolated. Additionally, SW can be harvested and used directly, unlike wastes from food crop whose availability depend on the abundance of the food crop itself and upon processing the crop. Thus, SW stands to be a cheaper source of cellulose. Initial study on the chemical composition of SW revealed that it contains 25–40% cellulose [29]. This suggests it is a good biomass for the production of CNSs and an added commercial value in waste management.

In the present study, we are reporting isolation of cellulose from the poisonous SW, transformation of the isolated cellulose into nanocrystal by acid hydrolysis and characterisation of the prepared CNSs.

2. Materials and methods

2.1. List of materials

Stems of SW were harvested from open bushy farmlands within an Estate along the Federal Polytechnic road, Ado-Ekiti, Nigeria. The following chemicals were used: sodium chlorite (Molychem), glacial acetic acid, sulphuric acid and ethanol (JHD), sodium hydroxide (BDH).

2.2. Preparation of CNC

2.2.1. Isolation of chemically purified cellulose (CPC)

Stems of SW were collected, dried, pulverized and sieved over 0.8 μm mesh size sieve. The pulverized sample was thereafter subjected to chemical treatment for purification and isolation of cellulose with some modifications from previous reports [21,30]. Extractives were first removed under Soxhlet extraction for 8 h in ethanol. The extractive-free sample (10 g) was treated with 25 g sodium chlorite and 7.5 mL acetic acid in 500 mL hot distilled water with stirring at 70 °C for 1 h. Thereafter, the same quantity of sodium chlorite and acetic acid was added, stirred for 1 h and the step repeated until a white coloured holocellulose was obtained. The mixture was filtered and washed with about 800 mL distilled water until the pH was 7 and then oven dried at 105 °C for 3 h. The resulting material, holocellulose (whitish in colour), is composed of hemicellulose and cellulose. The procedure was repeated until 50 g extractive-free sample was bleached. The bleached sample (15 g) was reacted with 20% NaOH solution in the ratio of (1:20) at 90 °C for 90 min after which the resulting mixture was allowed to cool down, filtered, washed to pH 7.7 and then oven dried at 105 °C for 3 h. The final dried product is considered as chemically purified cellulose – Siam weed (CPC-SW). Percentage yield of CPC-SW was determined gravimetrically.

2.2.2. Preparation of CNCs

CPC (9 g) was treated with 65 wt% sulphuric acid (cellulose to acid ratio 1:20) for 60 min at 45 °C under vigorous stirring. The reaction was quenched by pouring the hydrolysed cellulose into about 600 ml chilled distilled water, and thereafter centrifuged at 3000 rpm for 30 min. The aliquot gotten after centrifugation was dialysed against distilled water for 2 weeks until neutrality, and thereafter sonicated for 30 min in ice bath. The resulting suspension was freeze-dried to yield cellulose nanocrystals (CNC-SW) powder.

2.3. Characterization of SW and its CNC

2.3.1. Analysis of the chemical components

The content of extractives, holocellulose and cellulose present in the SW were calculated using the Technical Association of Pulp and Paper Industry (TAPPI) standards: T204 om-97, T19m-54, T203 OS-74. The difference between holocellulose and cellulose determines the hemicellulose content. The lignin content was determined gravimetrically assuming that extractives, hemicellulose and

cellulose are the only components of the entire SW.

2.3.2. Thermo-gravimetric analysis (TGA)

The thermal degradation and decomposition behaviour of the raw SW and its CNCs was observed with a Thermo-gravimetric Analyser (PerkinElmer, Llantrisant, Wales, UK) under a continuous nitrogen gas flow. 5.8 mg of the sample was placed in an aluminium pan and heated at a temperature range of 30–900 °C, with a heating rate of 10 °C/min under nitrogen atmosphere.

2.3.3. Fourier transformed infrared analysis (FTIR)

FTIR of the samples was recorded in transmittance mode using (PerkinElmer spectrum 100, Llantrisant, Wales, U.K.), employing a single reflection diamond MIRTGS detector. The wavenumber with which the analysis was carried out ranges from 650 to 4000 cm^{-1} with a resolution of 4 cm^{-1} and 64 scans per spectrum.

2.3.4. X-ray diffraction analysis (XRD)

The crystalline structure of SW and CNCs was measured on a Rigaku 600 X-ray Diffractometer (Japan) equipped with Cu-Kα radiation ($\lambda = 1.54056$ A°). The parameters used to obtain the diffractogram are: scan axis = theta/2-theta scan range of 0–90°, scan step of 0.1 and scan speed of 2.0°/min. the voltage and current was set to 40 kV and 15 mA respectively. The crystallinity index (CI) was calculated with OriginPro 8.5 using the equation below:

$$CI\ (\%) = \frac{Area\ of\ crystalline\ peak}{Area\ of\ crystalline\ and\ amorphous\ peaks} \times 100 \quad (1)$$

The cellulose size was determined using Scherrer's equation

$$Crystal\ size\ L = \frac{k\lambda}{\beta \cos\theta} \quad (2)$$

where K is the Scherrer constant 0.94, λ is 0.15406 Å, β is full width at half maximum (FWHM) and θ is the peak.

2.3.5. Scanning electron microscopy

In order to investigate the morphology of the SW and CNC-SW. The sample was placed onto an aluminium specimen stub covered with a double-sided carbon adhesive disc and sputter-coated with both palladium and gold for 4 min at 20 kV using scanning electron

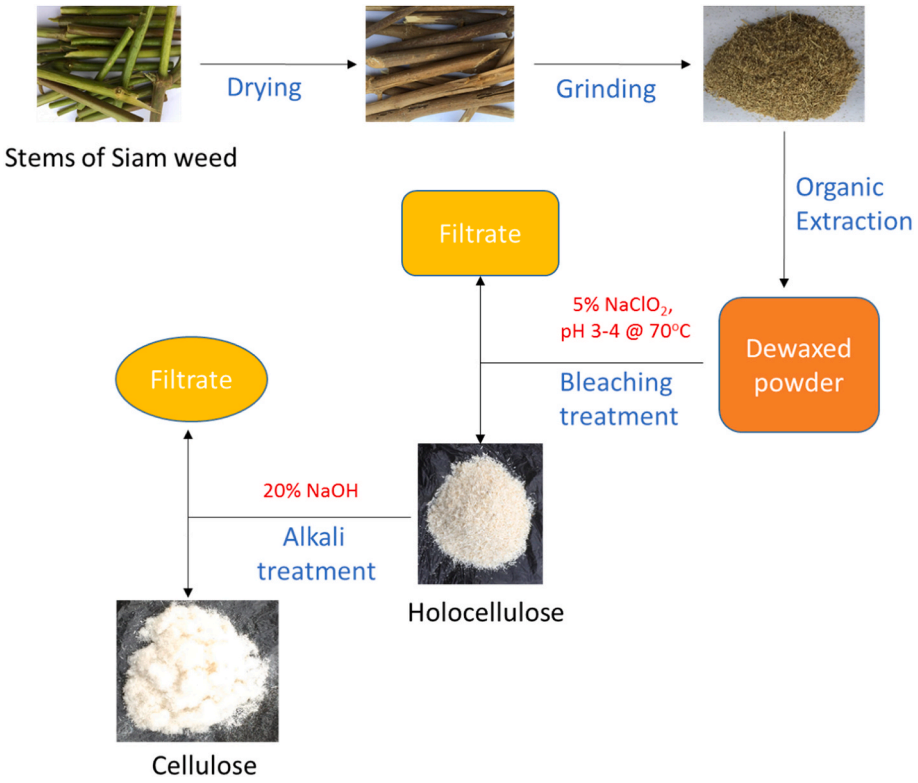

Fig. 1. Processes involved in the preparation of cellulose from Siam weed stems.

microscope (SIGMA VP, ZEISS Electron Microscopy, Carl Zeiss Microscopy Ltd; Cambridge, UK).

2.3.6. Transmission electron microscopy

The morphology and size of the nanoparticles were further confirmed using Transmission Electron Microscopy (TEM) (FEI Tecnai T12 TEM, 60–120 kV, Hillsboro, OR, USA). CNC-SW powder (1 mg) was dispersed in double deionized water and the suspension dropped on a Form Var® coated 200-mesh copper grip (TAAB Labs Equipment Ltd., Aldermaston, England) and allowed to dry at room temperature prior to TEM analyses [31].

2.3.7. Dynamic light scattering measurement

A Zetasizer Nano ZS (Malvern Instruments, Worcestershire, UK) was used to evaluate the hydrodynamic size and zeta potential of CNC-SW. Sample (1 mg) was dispersed in 2 mL doubled deionized water and sonicated for 30 s before being transferred into polystyrene cuvettes to measure the average particle size recorded at room temperature [31].

3. Results and discussion

3.1. Chemical composition of SW

The pulverized SW was sieved in order to maintain the size homogeneity of powdered stems. Thereafter, isolation of cellulose was carried out using multiple treatments as shown in Fig. 1. The organic extraction which is the first treatment was done in order to remove extractives and for the determination of the extractives, ethanol-cyclohexane (1:2) and ethanol alone, was used as solvents as against the conventionally used benzene. Both ethanol and cyclohexane are greener solvents compared to benzene which is carcinogenic. A previous study showed that extractive yield by ethanol-cyclohexane mixture is close to that obtained when ethanol-benzene mixture is used [25]. Initial attempt showed that the two solvents (ethanol-cyclohexane mixture and ethanol) gave the same yield of 4.2% extractives. Therefore, ethanol alone was used for extractive determination in this study. The first treatment was followed by bleaching treatment which is also known as delignification. The treatment at this stage removed lignin (which makes plants rigid) and the product obtained was a white-coloured holocellulose. Holocellulose comprises of hemicellulose and cellulose. Hence, the third treatment, which is the alkali treatment of the holocellulose was done using sodium hydroxide in other to remove the hemicellulose to obtain CPC-SW.

Results for the analysis of the chemical compositions of CPC-SW are presented in Table 1. CPC-SW contains 39.6% cellulose, 27.5% hemicellulose, 28.7% lignin and 4.2% extractives. The obtained values are in agreement with previously reported studies [29,32]. From Table 1, the significant difference in the cellulose values obtained is due to the fact that the present study and Ayeni and co-workers used only the stems of the plant [32] while Ogunjobi and co-workers used the whole biomass, that is, both leaves and stems [29]. This is so because composition of biomass differs depending on the procedures used for analysis, the location of the biomass geographically, differences in the solvents used, the particular part of the plant used in the compositional analysis. The percentage of the cellulose extracted shows that SW would be a very good source of cellulose and CNCs. Since cellulose has many active O–H groups, it can be easily modified.

A quick comparison of the chemical composition results of nanocellulose prepared from other agricultural wastes (jackfruit, groundnut and walnut) with SW as shown in Table 2, revealed that SW recorded the highest amount of isolated cellulose (39.6%) followed by groundnut (38.31%), walnut (27.4%) and then jackfruit (20.08%). With cellulose content of 60%–90% found in most of the cellulose-rich plants such as cotton seed, hemp and jute, it implies that SW possesses half of their cellulose content. The hemicellulose content of SW was relatively lower than found in walnut and groundnut but higher than found in jackfruit. Interestingly, jackfruit recorded the lowest amount of lignin (1.85%), more than twenty times less than found in SW. However, jackfruit peels are rich in extractives and contain ten times more than what was found in walnut and SW (Table 2).

The treatment procedure for the preparation of CNC is shown in Fig. 2 where CPC-SW was subjected to 65 wt% sulphuric acid hydrolysis for 1 h at 45 °C with vigorous stirring in order to break the amorphous region of the cellulose. Centrifugation, dialysis and sonication followed by freeze-drying of the resulting suspension afforded CNC, which was then characterised with spectroscopic, thermo-gravimetric and microscopic techniques.

3.2. FTIR analysis of SW and CNCs

FTIR spectra for SW and its CNC are presented in Fig. 3. In the spectrum of SW, there is a peak at 3312 cm^{-1} assigned to the O–H stretching vibration of the hydrogen-bonded hydroxyl group in the cellulose molecule. *C*–H stretching groups of cellulose appeared at 2894 cm^{-1} while C═O stretching frequency of ester group and stretching vibration of aromatic ring in lignin, hemicellulose and other

Table 1
Percentage composition of lingo-cellulosic biomass of SW.

Biomass	Cellulose (%)	Hemicellulose (%)	Lignin (%)	Extractive (%)	Reference
SW	39.60	27.50	28.70	4.20	present work
SW	40.20	29.90	23.20	4.80	[32]
SW	25.35	–	27.37	4.96	[29]

Table 2
Comparison between the properties of nanocellulose prepared from other agro-wastes and SW.

Property	Jackfruit	Groundnut	Walnut	Siam Weed
Cellulose	20.08%	38.31%	27.40%	39.60%
Hemicellulose	24.04%	27.62%	31.30%	27.50%
Lignin	1.85%	21.10%	36.30%	28.70%
Extractive	52.18%	–	1.57%	4.20%
Crystal size	2.80 nm	4.20 nm	–	2.20 nm
Crystallinity index	83.42%	74.00%	42.90%	66.20%
References	[23]	[21]	[22]	Present study

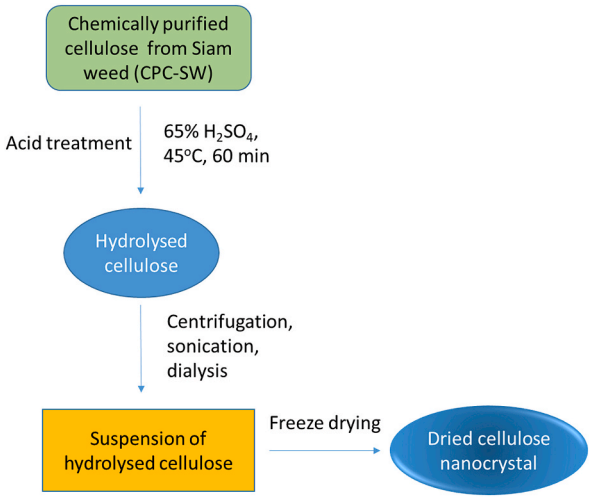

Fig. 2. Schematic diagram for the preparation of CNC from CPC-SW.

component appeared at 1723 cm^{-1} and 1253 cm^{-1}. The peak at 1515 cm^{-1} is assigned to the C═C of the aromatic ring of lignin and also, H–*O*–H bending vibration of absorbed water at 1642 cm^{-1} is due to the hydroxyl groups in cellulose. In the spectrum of CNC, there is an increase in the band of the O–H group (3330 cm^{-1}) which is characteristic of CNCs [33]. The *C*–H stretching group is also present at 2915 and 2846 cm^{-1}. The complete disappearance of the bands at 1723 cm^{-1}, 1253 cm^{-1}, 1515 cm^{-1} confirmed the removal of lignin, hemicellulose and other components. The appearance of a small peak at 1205 cm^{-1} is assigned to S═O vibration of sulphate group (from the hydrolysis of the cellulose using sulphuric acid) [34]. The bands at 1468 cm^{-1} is assigned $-CH_2$-(C_6)-bending, 1596 cm^{-1} is assigned *C*–C vibration in aromatic ring, while 1033 cm^{-1} is assigned to *C*–*O*–C stretching of 1,4-glycosidic linkages of the D-glucose units in cellulose. These peaks (1468 cm^{-1}, 1596 cm^{-1} and 1033 cm^{-1}) are interpreted for cellulose structure [35].

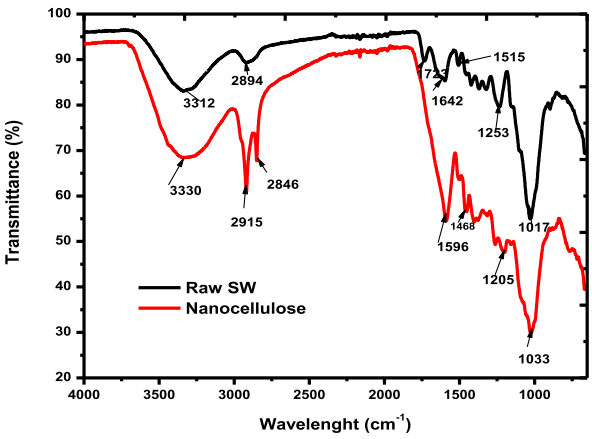

Fig. 3. FTIR spectra of SW (black) and the prepared CNC-SW (red).

3.3. TGA analysis of SW and CNC-SW

TGA-DTG curves of SW and nanocellulose prepared from it are shown in Fig. 4. A three-step degradation occurred on the thermograms and this agrees with the literature [21]. The significant weight loss below 110 °C was due to loss of absorbed water. The second step is indicated by endothermic peaks between 200 and 350 °C involving degradation of the cellulosic chain which corresponded with hemicellulose degradation and the beginning of lignin degradation [36]. The third step degradation occurred at around 400 °C on SW while on CNC it occurred at 450 °C. At this stage, the carbonic residue decomposed into low molecular weight compound. The higher temperature of degradation exhibited by CNC indicates a higher average kinetic energy. The several crystalline regions in the CNC are a predictor of high thermal stability [22]. This outcome agrees with the result obtained from XRD analyses presented in Fig. 5. More so, the lower thermal stability of the raw SW when compared with CNC is as a result of the presence of the non-cellulosic component with lower temperature of degradation [37].

3.4. XRD analysis of SW and its CNCs

Diffractograms of raw SW and the CNC prepared from it are shown in Fig. 5. The XRD spectra show two distinct peaks at 22.6° and 34.88°. These peaks have been reported to characterize cellulose crystal assigned for 200 and 004 planes [21]. Since SW is a carbonaceous material, its CNCs is a polymer of carbon as observed in the XRD pattern. The crystallinity index (CI) was calculated from equation (1) and further processed on OriginPro 8.5 software. CI of CNC was found to be 66.2% while SW has CI of 30.5%. The sharp distinct peak shown at 47.5° on the CNC diffractogram proves the role of chemical treatment (acid hydrolysis) that increased crystallinity of CNC while removing the amorphous region. This result shows an increase in crystallinity after multiple treatments on SW to produce CNC. The crystal size calculated for the cellulose nanocrystals using Scherrer's formula from equation (2) was found to be 2.2 nm.

The CI and the crystal size of nanocellulose from other biomass are presented in Table 2. It is obvious that jackfruit and groundnut nanocelluloses have bigger crystal size and are clearly more crystalline than nanocellulose from SW in this study.

3.5. SEM, TEM and DLS analysis

SEM provides information on the surface morphology and microstructure of the samples: raw SW and CNCs. SEM resolves both the chemical and structural features at high resolution. The micrograph of SW in Fig. 6(a), at a magnification of ×600, showed that there is surface compactness due to the binding together of lignin, hemicellulose, other components and several amorphously shaped structures in the raw SW. At a magnification of ×8960, there is a large hollow pit embedded with fairly interlocking fibres (Fig. 6(b)). The surface also appeared to have a smooth texture. In Fig. 6(c), the surface compactness has become loosed indicating that degradation of cellulosic chain has occurred alongside removal of the binding components. There is an obvious and well-marked reduction in particle size and diameter of the CNCs (at the same magnification of ×600) when compared with the size of the raw sample in the micrograph in Fig. 6(a). On a scale of 10 μm and at ×4330, certain nanospheres are seen (Fig. 6(d)), thus having a higher surface area than the SW shown in Fig. 6(a).

TEM micrographs at the scale of 200 nm (Fig. 6(e)) and 100 nm (Fig. 6(f)) show the spherically shaped CNC-SW having an average particle size <100 nm. The presence of spherical crystals results from acid hydrolysis of the isolated cellulose leading to soft, non-clustered non-fibrous uniform nano-dimensioned crystals from SW. By the developed method, the geometry of CNCs obtained from SW is similar to those from jack fruit peel [23].

DLS studies revealed CNC-SW size distribution as shown in Fig. 6(g). The hydrodynamic size was measured at an average of 213 nm while the nanocellulose had an overall negatively charged surface with a zeta potential value of −9.57 mV (Fig. 6 h). Nanocelluloses

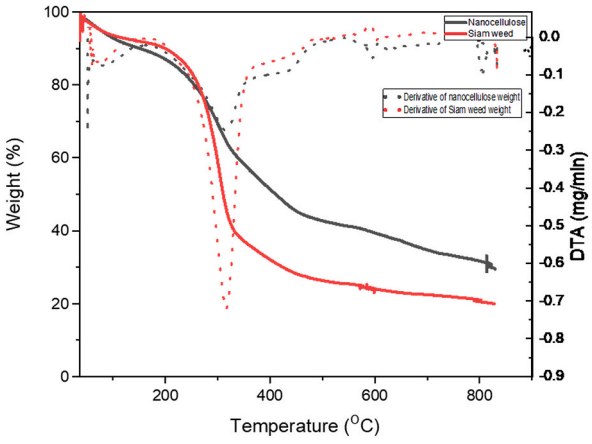

Fig. 4. TGA-DTG curves for raw SW and CNC-SW.

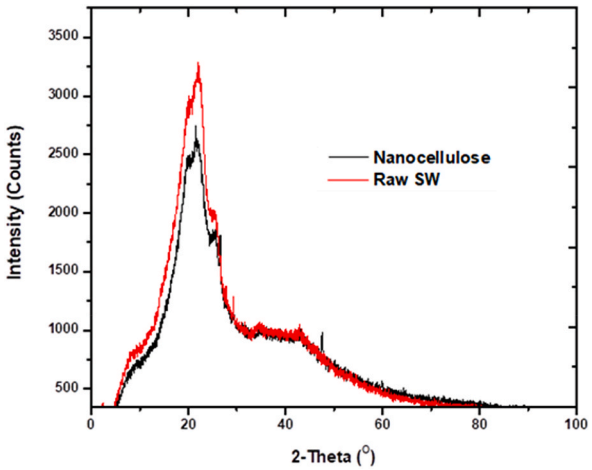

Fig. 5. XRD analysis for raw SW and CNC-SW.

are known to have large surface area that are negatively charged [23,38].

4. Conclusion

Cellulose has been successfully isolated in good yield (~40%) from the abundant but persistent, invasive Siam weed threatening agricultural production and livestock in our environment. The amount of cellulose isolated is more than what has been obtained from many other non-woody sources. CNC was prepared from the isolated cellulose using acid hydrolysis method and structurally confirmed by FTIR. Microscopic and thermo-gravimetric characterization of the CNC revealed the nanocellulose has a relatively high crystallinity and a fairly high thermal stability when compared with the weed. This is typical of a well-isolated CNC as reported in the literature. Morphological characterisation with SEM and TEM and particle size distribution measurement through DLS revealed that the nanocellulose prepared are uniformly distributed spherically shaped nanocrystals with an average hydrodynamic size of 213 nm and are negatively charged at −9.57 mV. Additionally, a greener solvent (ethanol) was used as a substitute to ethanol-cyclohexane mixture as well as benzene in the removal of extractives from the biomass. This affords a cheaper, cleaner and safer pre-treatment process for the biomass. As such, the extraction method presented in this report is eco-friendly and a hand-on experimental technique for the synthesis of nanocellulose. Attempts to apply the prepared CNC in environmental remediation and water purification is underway.

Author contribution statement

Joseph Kolawole Ogunjobi: Conceived and designed the experiments; Analyzed and interpreted the data; Contributed reagents, materials, analysis tools or data; Wrote the paper.

Adetola Ibukunoluwa Adewale: Conceived and designed the experiments; Performed the experiments; Analyzed and interpreted the data; Contributed reagents, materials, analysis tools or data; Wrote the paper.

Samson Adebowale Adeyemi: Analyzed and interpreted the data; Contributed reagents, materials, analysis tools or data.

Funding statement

Authors did not receive any grant from funding agencies in the public, commercial, or not-for-profit sectors for this study.

Data availability statement

Data will be made available on request.

Declaration of interest's statement

The authors declare no competing interests.

Abbreviations

SW	Siam weed
CPC	Chemically purified cellulose
CNC	Cellulose nanocrystals

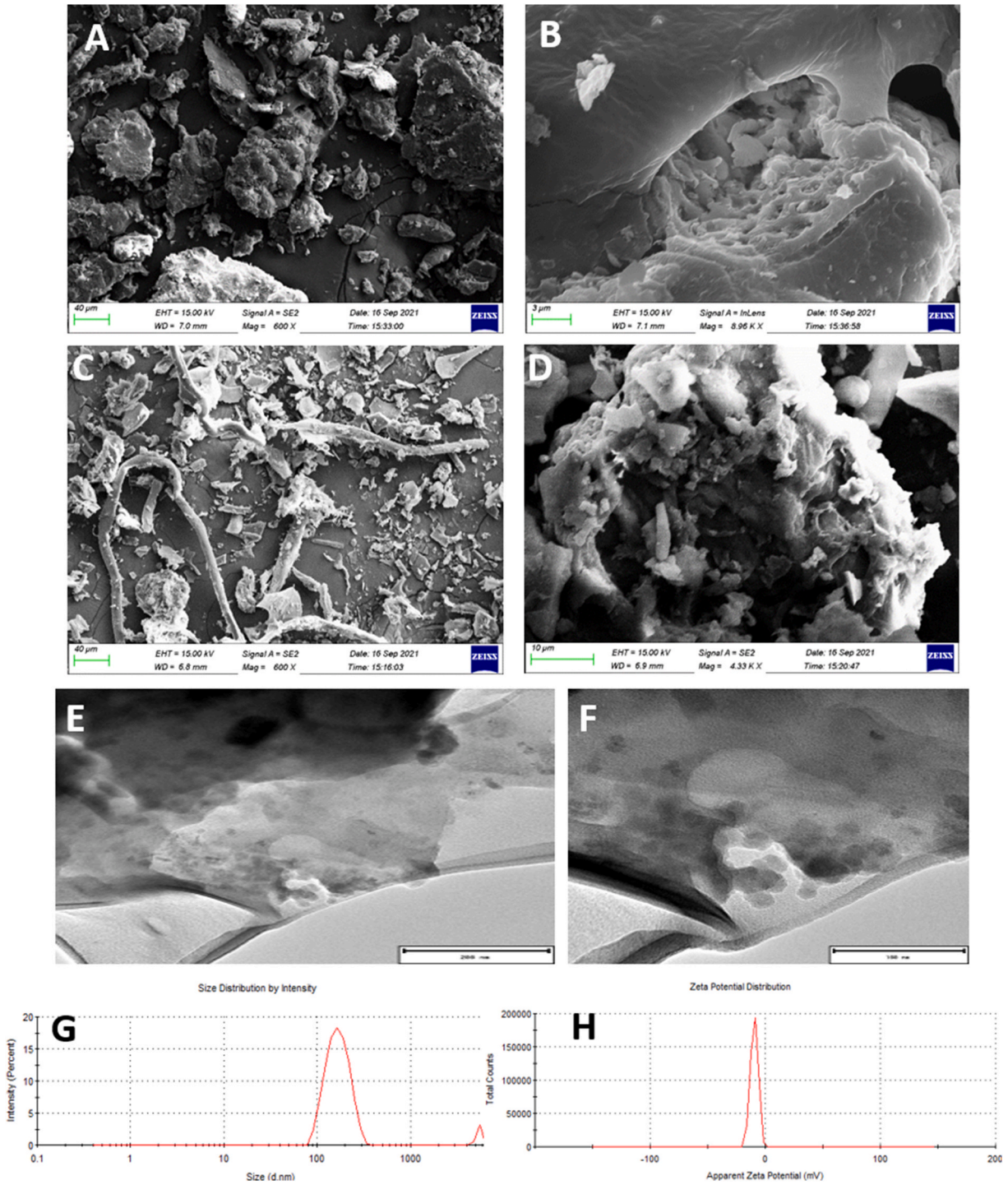

Fig. 6. SEM micrographs (a) raw pulverized SW stems with magnification of ×600 (b) raw pulverized SW stems with magnification of ×8960 (c) isolated CNCs with magnification of ×600 and (d) isolated CNCs with magnification of ×4330. TEM micrographs (e and f) TEM micrographs of CNC-SW show uniform spherical crystals of average size <100 nm in line with SEM images. DLS (g) Average zeta size of CNC-SW. Average hydrodynamic size of CNC-SW was about 213 nm (h) Average zeta surface potential of CNC-SW. CNC-SW surface was found to be charged at –9.57 mV.

References

[1] E. Kontturi, et al., Advanced materials through assembly of nanocelluloses, Adv. Mater. 30 (24) (2018), 1703779.
[2] C. Moreau, et al., Tuning supramolecular interactions of cellulose nanocrystals to design innovative functional materials, Ind. Crop. Prod. 93 (2016) 96–107.

[3] M. Pitkanen, et al., Nanofibrillar Cellulose: in Vitro Study of Cytotoxic and Genotoxic Properties, TAPPI Press, 2010.
[4] M. Borjesson, G. Westman, Crystalline nanocellulose—preparation, modification, and properties, Cellulose-Fund. Asp. Curr. Trends 7 (2015).
[5] H.P.S.A. Khalil, A.H. Bhat, A.F.I. Yusra, Green composites from sustainable cellulose nanofibrils: a review, Carbohydr. Polym. 87 (2) (2012) 963–979.
[6] M. Kaushik, A. Moores, Nanocelluloses as versatile supports for metal nanoparticles and their applications in catalysis, Green Chem. 18 (3) (2016) 622–637.
[7] J.D.P. de Amorim, et al., Plant and bacterial nanocellulose: production, properties and applications in medicine, food, cosmetics, electronics and engineering. A review, Environ. Chem. Lett. 18 (3) (2020) 851–869.
[8] P. Phanthong, et al., Nanocellulose: extraction and application, Carbon Res. Conv. 1 (1) (2018) 32–43.
[9] N. Tapia-Orozco, et al., Removal strategies for endocrine disrupting chemicals using cellulose-based materials as adsorbents: a review, J. Environ. Chem. Eng. 4 (3) (2016) 3122–3142.
[10] Z. Karim, et al., High-flux affinity membranes based on cellulose nanocomposites for removal of heavy metal ions from industrial effluents, RSC Adv. 6 (25) (2016) 20644–20653.
[11] J. Liu, S. Willfor, A. Mihranyan, On importance of impurities, potential leachables and extractables in algal nanocellulose for biomedical use, Carbohydr. Polym. 172 (2017) 11–19.
[12] X. Du, et al., Nanocellulose-based conductive materials and their emerging applications in energy devices-A review, Nano Energy 35 (2017) 299–320.
[13] N. Hasan, et al., Recent advances of nanocellulose in drug delivery systems, J. Pharm. Investig. 50 (6) (2020) 553–572.
[14] S. Fujisawa, E. Togawa, K. Kuroda, Facile route to transparent, strong, and thermally stable nanocellulose/polymer nanocomposites from an aqueous Pickering emulsion, Biomacromolecules 18 (1) (2017) 266–271.
[15] H. Kargarzadeh, et al., Recent developments on nanocellulose reinforced polymer nanocomposites: a review, Polymer 132 (2017) 368–393.
[16] C. Wan, et al., Ultralight and hydrophobic nanofibrillated cellulose aerogels from coconut shell with ultrastrong adsorption properties, J. Appl. Polym. Sci. 132 (24) (2015).
[17] B.-H. Cheng, R.J. Zeng, H. Jiang, Recent developments of post-modification of biochar for electrochemical energy storage, Bioresour. Technol. 246 (2017) 224–233.
[18] M. Roman, et al., Cellulose Nanocrystals for Drug Delivery, ACS Publications, 2009.
[19] M. Tavakolian, et al., Dye removal using hairy nanocellulose: experimental and theoretical investigations, ACS Appl. Mater. Interfaces 12 (4) (2019) 5040–5049.
[20] Y.-L. Hsieh, Cellulose nanocrystals and self-assembled nanostructures from cotton, rice straw and grape skin: a source perspective, J. Mater. Sci. 48 (22) (2013) 7837–7846.
[21] S. Bano, Y.S. Negi, Studies on cellulose nanocrystals isolated from groundnut shells, Carbohydr. Polym. 157 (2017) 1041–1049.
[22] D. Zheng, et al., Isolation and characterization of nanocellulose with a novel shape from walnut (Juglans regia L.) shell agricultural waste, Polymers 11 (7) (2019) 1130.
[23] C. Trilokesh, K.B. Uppuluri, Isolation and characterization of cellulose nanocrystals from jackfruit peel, Sci. Rep. 9 (1) (2019) 1–8.
[24] C.C. Hernandez, F.F. Ferreira, D.S. Rosa, X-ray powder diffraction and other analyses of cellulose nanocrystals obtained from corn straw by chemical treatments, Carbohydr. Polym. 193 (2018) 39–44.
[25] J.K. Ogunjobi, O.M. Balogun, Isolation, modification and characterisation of cellulose from wild Dioscorea bulbifera, Sci. Rep. 11 (1) (2021) 1025.
[26] B.S.L. Brito, et al., Preparation, morphology and structure of cellulose nanocrystals from bamboo fibers, Cellulose 19 (5) (2012) 1527–1536.
[27] J.I. Moran, et al., Extraction of cellulose and preparation of nanocellulose from sisal fibers, Cellulose 15 (1) (2008) 149–159.
[28] Chromolaena odorata, Global Invasive Species Database, 2022 [cited 2022 27-10-2022]; Available from: http://www.iucngisd.org/gisd/speciesname/Chromolaena+odorata.
[29] J.K. Ogunjobi, L. Lajide, B.J. Owolabi, Conversion of Siam weeds and rice straws to energy products and valuable chemicals via pyrolysis, Int. J. Environ. Waste Manag. 17 (2) (2016) 91–102.
[30] M.A. Adekoya, et al., Structural characterization and solid state properties of thermal insulating cellulose materials of different size classifications, Bioresources 13 (1) (2018) 906–917.
[31] S.A. Adeyemi, et al., Folate-decorated, endostatin-loaded, nanoparticles for anti-proliferative chemotherapy in esophaegeal squamous cell carcinoma, Biomed. Pharmacother. 119 (2019), 109450.
[32] A.O. Ayeni, et al., Compositional analysis of lignocellulosic materials: evaluation of an economically viable method suitable for woody and non-woody biomass, Am. J. Eng. Res. 4 (4) (2015) 14–19.
[33] N. Raghav, M.R. Sharma, J.F. Kennedy, Nanocellulose: a mini-review on types and use in drug delivery systems, Carbohyd. Polym. Technol. Appl. 2 (2021), 100031.
[34] H.A. Silverio, et al., Extraction and characterization of cellulose nanocrystals from corncob for application as reinforcing agent in nanocomposites, Ind. Crop. Prod. 44 (2013) 427–436.
[35] F. Luzi, et al., Valorization and extraction of cellulose nanocrystals from North African grass: ampelodesmos mauritanicus (Diss), Carbohydr. Polym. 209 (2019) 328–337.
[36] R.A. Ilyas, S.M. Sapuan, M.R. Ishak, Isolation and characterization of nanocrystalline cellulose from sugar palm fibres (Arenga Pinnata), Carbohydr. Polym. 181 (2018) 1038–1051.
[37] H. Yang, et al., Characteristics of hemicellulose, cellulose and lignin pyrolysis, Fuel 86 (12–13) (2007) 1781–1788.
[38] M.R.K. Sofla, et al., A comparison of cellulose nanocrystals and cellulose nanofibres extracted from bagasse using acid and ball milling methods, Adv. Nat. Sci. Nanosci. Nanotechnol. 7 (3) (2016), 035004.